ChemComm

Accepted Manuscript

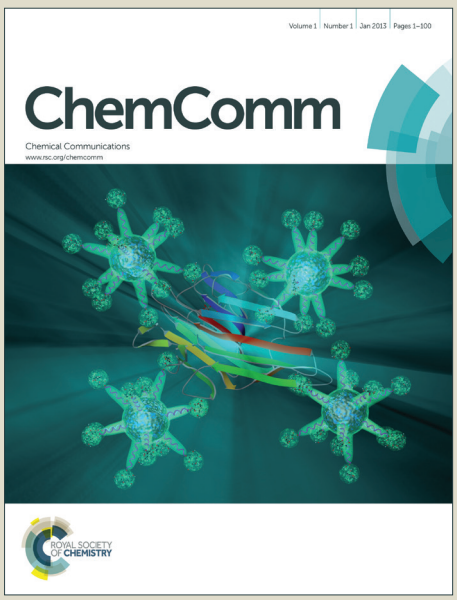

ROYAL SOCIETY OF CHEMISTRY

www.rsc.org/chemcomm

ChemComm

Dynamic Article Links ►

Cite this: DOI: 10.1039/coxx00000x

www.rsc.org/xxxxxx

COMMUNICATION

Three-dimensional porous stretchable and conductive polymer composites based on graphene network grown by chemical vapour deposition and PEDOT:PSS coating

Mengting Chen, Shasha Duan, Ling Zhang,* Zhihui Wang and Chunzhong Li*

Received (in XXX, XXX) Xth XXXXXXXXX 20XX, Accepted Xth XXXXXXXXX 20XX
DOI: 10.1039/b000000x

We have manufactured a highly conductive and stretchable composite by backfilling the 3D graphene-PEDOT:PSS skeleton with poly(dimethylsiloxane) (PDMS). The electrical conductivity of our product can reach 24 S cm^{-1} with only 1.5 wt% graphene and 1.5 wt% PEDOT:PSS loading, and its resistance only increased 35% when stretched to 80% strain.

Stretchable conductive materials (SCMs) can enable a spectrum of applications in next-generation smart electronics such as wearable electronics, smart clothing, E-skins and so on.[1-3] To fabricate SCMs successfully, one general and effective approach is to introduce conductive fillers into elastomeric matrix.[4-9] Among these fillers, graphene has been extensively explored on account of its superior electrical and mechanical properties.[3,10] At present, the most widely used method to produce graphene is chemical reduction of exfoliated graphene oxide (RGO). However, two drawbacks have limited the application of RGO in SCMs: structural defects and easily agglomerated in matrix.[3,11,12] Fortunately, graphene grown by CVD method possesses intact structure, producing ideal quality such as higher conductivity, which makes it a better candidate than RGO in the applications of SCMs. Nevertheless, two challenges within CVD graphene still limited its applications, which are the residues after the transfer process and unstable doping.[13-17] When PEDOT:PSS is introduced into CVD graphene, it works as both supporting layer and dopant,[18] and thus these two problems get resolved favorably. Therefore, the combination of CVD graphene and PEDOT:PSS would endows SCMs with better electrical property. Despite high conductivity, another critical factor for high-performance SCMs is good conductivity retention capability under large deformation, and previous studies have verified that SCMs with three-dimensional (3D) porous structure could not only overcome the dispersion problem of graphene, but also show excellent conductivity retention rate, which is of great significance in the prospective applications of SCMs.[1,3,10] Hence, it is a good choice to prepare a high performance SCM – combining the 3D graphene that grown by CVD method and dopant PEDOT:PSS with porous polymer matrix.

Therefore, in this communication, we have demonstrated a novel strategy to fabricate a porous CVD graphene-PEDOT:PSS-PDMS (CGPP) composite for the application of SCMs. The graphene was grown on 3D nickel (Ni) foam (GF) and the covered PEDOT:PSS coating act as a dopant of it. Thus, when assembling this GF/PEDOT conductive network with a thin layer of PDMS, and after the etching process of Ni framework, the porous and stretchable conductive CGPP was successfully obtained. The CGPP possesses remarkable electrical conductivity and the ability to withstand large deformations. When the content of graphene and PEDOT:PSS are 1.5 wt% and 1.5 wt%, respectively, CGPP shows a very high electrical conductivity (24 S cm^{-1}), which is ~ 1.6 times higher than CVD graphene-PDMS (CGP, 3 wt% graphene loading, 15 S cm^{-1}) prepared as a reference. Moreover, when the composite was stretched to 80% strain, the resistance of CGPP only increased 20%.

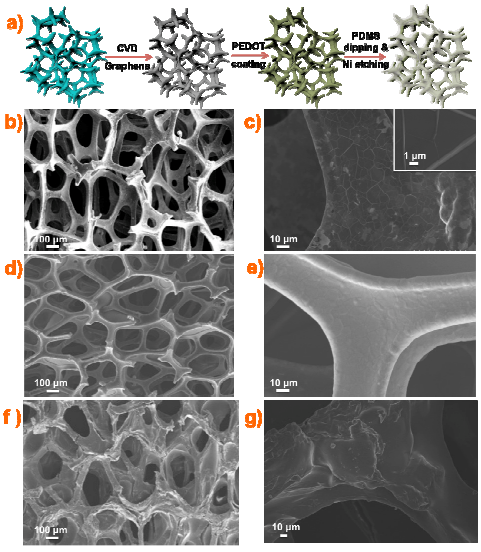

Fig. 1. a) Schematic illustration of CGPP preparation; FE-SEM images of b), c) Ni foam with graphene grown on it by CVD method and d), e) a thin layer of PEDOT:PSS coated on the GF; after backfilling the 3D graphene/PEDOT network with PDMS, the CGPP was obtained and its FE-SEM images were shown in f) and g).

The detailed experimental section is presented in ESI and the fabrication process is schematically illustrated in Fig. 1a. In brief, Ni foam with 3D interconnected structure served as a template, and a few layers of graphene sheets were grown on it by CVD method. Then, a thin, complete and uniform layer of PEDOT:PSS

was coated on these sheets with the aid of polyurethane (PU). The Ni/graphene/PEDOT framework was impregnated with a dilute PDMS organic solution, which acts as a supporting layer to protect the 3D conductive skeleton. Finally, the highly stretchable CGPP film was successfully obtained after etching the Ni away. In comparison, we also prepared CGP composite as the control sample, a porous SCM simply composed with CVD graphene and PDMS. The detailed fabrication process and structure is also present in ESI.

Fig. 1b shows the SEM image of graphene grown on Ni foam by CVD method. It can be seen that a comparatively uniform graphene cladding is coated on the surface of Ni foam scaffold thoroughly. Though some wrinkles caused by grain boundaries[19] of Ni appear on graphene sheets, no cracks can be observed (Fig. 1c), indicating that the conductive network of CVD graphene is coherent and complete. In addition, the Raman spectra measurement (Fig. S1c, ESI) illustrates that the graphene cladding grown on Ni foam consists of monolayer to few layers of graphene sheets. Therefore, the structural and dispersive problems of RGO used in SCMs would be successfully eliminated by the high-quality CVD graphene foam structure.

Then, a thin layer of PEDOT:PSS coating was introduced to further increase the electrical property of GF by doping mechanism. However, it was found that a large amount of cracks would emerge if GF was simply coated with pure aqueous solution of PEDOT:PSS (Fig. S2, ESI). This phenomenon is presumably because the evaporation rates (ER) of water in different regions of the 3D scaffold at 90℃ were diversely. The quicker ER would produce solid grain on the surface of PEDOT:PSS solution, which will impact the fluxion of solution and cause film defects. While when the water was replaced by high boiling point solvent like ethylene glycol (EG), the evaporation rates of EG would be more uniform, and there present no cracks in the coating. But another problem comes up that the PEDOT:PSS coating only covered the outside GF skeletons completely while partly smeared those inside regions. To overcome these issues, waterborne PU resin was added into aqueous solution of PEDOT:PSS to make the coating more uniformly and integrally with an equable ER. It is supposed that PU weakens the surface tension of PEDOT:PSS solution, and thus the wettability between PEDOT:PSS and graphene was improved significantly (Fig. S4, ESI). Thus, with only a small amount of PU (0.1 wt% in aqueous PEDOT:PSS solution), the whole 3D GF scaffolds was overlaid by PEDOT:PSS glossily and evenly, and no cracks appeared over all this framework (Fig. 1d and e).

After impregnating the fabricated G/PEDOT:PSS in a dilute PDMS organic solution and followed by curing at 100℃ for 30 min, a supporting thin layer of PDMS formed and the 3D scaffold was protected from collapsing. Then Ni was completely removed and the ultimate stretchable CGPP was successfully generated. As shown in the FE-SEM images of CGPP (Fig. 1f and g), the surface of CGPP is very smooth and no structural damage emerged after Ni etching-process. The acquired CGPP shows excellent electrical conductivity (24 S cm^{-1}), exhibiting much more higher value compared to CGP with the same content of graphene. The reason for this result comes from the synergetic graphene and PEDOT:PSS. The PEDOT:PSS layer plays the role of dopant and further improved the electrical property of CVD graphene. The doping effect could be interpreted as electron attraction and transfer more easier between CVD graphene and PEDOT:PSS.[15] Therefore, the obstacles for electrons transport could be reduced significantly compared to pure 3D graphene framework, endowing the CGPP with superior conductivity than CGP composites.

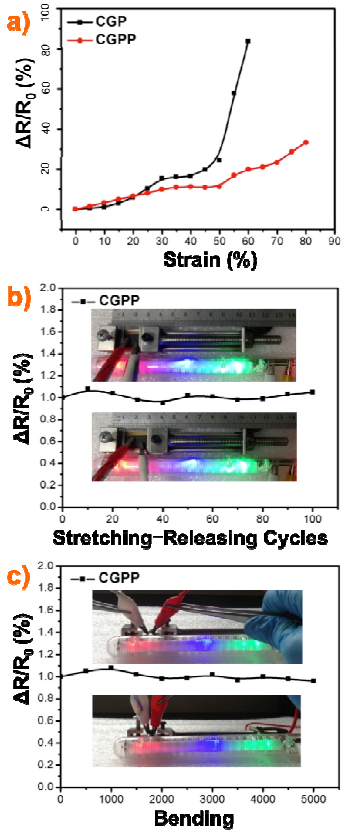

Fig.2. Electrical-resistance variation of: a) CGPP and CGP films as a function of tensile strain; b) CGPP film as a function of stretching-releasing cycles with 50% strain; c) CGPP film as a function of the number of bends. the inset photos in b) and c) are the brightness of LED lamps in series with CGPP depending on strains and bends, indicating minor resistance variations of CGPP after stretching and bending deformation.

To testify the properties of CGPP as a stretchable conductor in depth, both CGP and CGPP films were stretched to a series of certain present strains, and their electrical resistances were measured simultaneously. R_0 is recorded as the initial resistance of each film at zero strain and $\Delta R/R_0$ represents resistance variations as a function of the applied tensile strain. As shown in Fig. 2a, the resistances of both CGP and CGPP increased during the stretching process, and the increment of CGP is much greater than that of CGPP at larger strains. When strain is less than 20%, the resistances of these two films nearly have identical changing trends; while when the films were further stretched to larger than 20% strain, the $\Delta R/R_0$ of CGP increased more sharply than CGPP, especially at the strain beyond 50%. For example, as the strains for these films were increased to 60%, the $\Delta R/R_0$ of CGPP only exhibits a ~20% enhancement while of CGP is as high as 85%. These phenomena indicate that the dopant – PEDOT:PSS not only improves the electrical conductivity of the CGPP, but also has a positive effect on resistance retention capacity of CGPP under stretching. When the composites were stretched to a certain strain, the graphene sheets in these two films are starting to crack, and thus the resistance of CGP increased acutely. However, because of the PEDOT:PSS layer on the GF, the situation in CGPP is quite

different. The PEDOT:PSS coating was functioned as a conductive connection, and most of the cracks would be filled efficiently, the increment of resistance caused by 2D graphene was also being supplemented. Therefore, with the aid of PEDOT:PSS, the CGPP shows superior electrical performance than CGP in the SCMs.

Furthermore, the electrical properties of CGPP under cyclic mechanical deformations were also been investigated. As shown in Fig. 2b and c, the resistance of the composite almost kept stable during 5,000 times of bending and 100 cycles of 50% stretching-releasing process. The excellent durability of CGPP can be mainly attributed to the cooperative interaction between PEDOT:PSS and graphene, which plays a key role in keeping the conductive network connected under repeated deformations. What's more, the PDMS supporting layer combined with the conductive network tightly, when the strain was released, the relaxed polymer molecule chains would recover the sliding nanofilers' contact points that caused by mechanical deformations completely. Therefore, the brightness and color of LED lamps exhibited almost no change after stretching to 50% strain and bending curvature of 2 mm, which fitted well with the results of the $\Delta R/R_0$-stretching and $\Delta R/R_0$-bending curves. As demonstrated, the CGPP shows enormous potential in next-generation smart electronics that require bending and stretching durability.

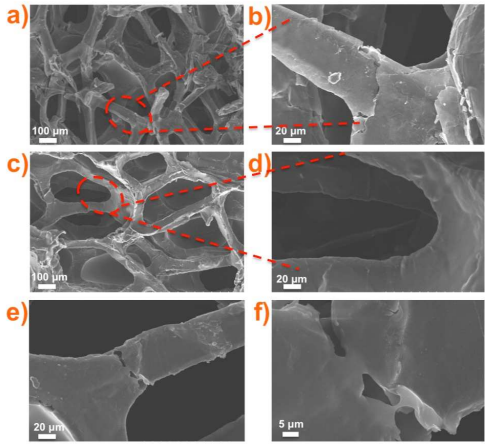

Fig.3. SEM images of CGP (a) and CGPP (c) under elongation of 60%; (b) and (d-f) are magnifications of (a) and (c), respectively.

To better understand the effect of PEDOT:PSS on the superior electrical performance of CGPP, both CGP and CGPP are stretched to 60% strain and their corresponding microstructures are present by SEM as shown in Fig. 3. For CGP, lots of cracks appear on the 3D scaffold at 60% elongation, which would break off the conductive path and resulting in inferior electrical property. However, with a thin layer of PEDOT:PSS coated on graphene, crevices can hardly be observed when the strain reached the same with CGP (60%, Fig. 3d). Compared with the totally separated structure in CGP (Fig. 3b), the rarely founded cracks present in CGPP still exist connections between two neighboring segments (Fig. 3f). This can be attributed to the introduction of PEDOT:PSS, which brought a close connection between conductive framework and PDMS (Fig. S5, ESI). As a result, compared to CGP, CGPP exhibited a much more pacific degradation of electrical property at the same degree of stretching.

In summary, highly conductive stretchable CGPP was prepared by combining CVD graphene/PEDOT:PSS with a 3D polymer skeleton. Due to the high conductivity of CVD graphene and PEDOT:PSS, and the doping effect introduced by the conducting polymer, the composite film shows high conductivity of 24 S/cm only with 1.5 wt% graphene and 1.5 wt% PEDOT:PSS loading. With such special-designed 3D conductive network, the CGPP exhibits both remarkable electrical conductivity and good resistance retention capability under deformations. The resistance retention rate of CGPP is 4 times lower than that of CGP. In addition, the resistance of CGPP remains stable even after stretching to 50% for 100 times and bending for 5000 times. The fascinating performance of CGPP will make a huge potential in the applications of next-generation stretchable electronics.

The authors are grateful to the National Natural Science Foundation of China (51173043, 21136006, 2123600, 21322607), the Special Projects for Nanotechnology of Shanghai (12nm0502700), the Basic Research Program of Shanghai (13JC1408100), the Key Scientific and Technological Program of Shanghai (14521100800), Program for New Century Excellent Talents in University (NCET-11-0641), the Fundamental Research Funds for the Central Universities.

Notes and References

Key Laboratory for Ultrafine Materials of Ministry of Education, School of Materials Science and Engineering, East China University of Science and Technology, 130 Meilong Road, Shanghai 200237, China. Fax: +86 21 64250624; Tel: +82 21 64252055; E-mail: czli@ecust.edu.cn

†Electronic Supplementary Information (ESI) available: Experimental details, Fig. S1-S7. See DOI:

1 M. Chen, T. Tao, L. Zhang, W. Gao and C. Li, Chem. Comm., 2013, 49, 1612-1614.
2 M. Chen, L. Zhang, S. Duan, S. Jing, H. Jiang, M. Luo and C. Li, Nanoscale, 2014, 6, 3796-3803.
3 M. Chen, L. Zhang, S. Duan, S. Jing, H. Jiang and C. Li, DOI: 10.1002/adfm201401886.
4 F. Xu, and Y. Zhu, Adv. Mater., 2012, 24, 5117-5122.
5 H. Stoyanov, M. Kollosche, S. Risse, R. Waché and G. Kofod, Adv. Mater., 2013, 25, 578-583.
6 D. Wang, H. Li, M. Li, H. Jiang, M. Xia, and Z. Zhou, J. Mater. Chem. C., 2013, 1, 2744-2749.
7 S. Kim, J. Byun, S. Choi, D. Kim, T. Kim, S. Chung and Y. Hong, Adv. Mater., 2014, 26, 3094-3099.
8 M. Li, H. Li, W. Zhong, Q. Zhao and D. Wang, Acs Appl. Mater. Interfaces, 2014, 6, 1313-1319.
9 J. Ge, H. Yao, X. Wang, Y. Ye, J. Wang, Z. Wu, J. Liu, F. Fan, H. Gao, C. Zhang and S. Yu, Angew. Chem. Int. Ed., 2013, 52, 1654-1659.
10 Z. Chen, W. Ren, L. Gao, B. Liu, S. Pei and H. Cheng, Nature Materials, 2011, 10, 424-428.
11 K. S. Novoselov, A. K. Geim, S. V. Morozov, D. Jiang, Y. Zhang, S. V. Dubonos, I. V. Grigorieva, A. A. Firsov, Science, 2004, 306, 666-669.
12 C. Zhu, S. Guo, Y. Fang and S. Dong, ACS NANO, 2010, 4, 2429-2437.
13 L. G. De Acro, Y. Zhang, C. W. Schlenkev, K. Ryu, M. E. Thompson and C. Zhou, ACS NANO, 2010, 5, 2865-2873.
14 B. H. Lee, J-H. Lee, Y. H. Kahng, N. Kim, Y. J. Kim, J. Lee, T. Lee and K. Lee, Adv. Funct. Mater., 2014, 24, 1847-1856.
15 D. Wei, Y. Liu, Y. Wang, H. Zhang, L. Huang and G. Yu, Nano Lett., 2009, 9, 1752-1758.
16 C. Zhang, L. Fu, N. Liu, M. Liu, Y. Wang and Z. Liu, Adv. Mater., 2011, 23, 1020-1024.
17 Y. Kim, J. Ryu, M. Park, E. S. Kim, J. M. Yoo, J. Park, J. H. Kang and B. H. Hong, ACS NANO, 2014, 1, 868-874.
18 M. Vosgueritchian, D. J. Lipomi and Z. Bao, Adv. Funct. Mater., 2012, 22, 421-428.
19 C. Jeong, P. Nair, M. Khan, M. Lundstrom and M. A. Alan, Nano Lett., 2011, 11, 5020-502